The cytosolic tail dipeptide Ile-Met of the pea receptor BP80 is required for recycling from the prevacuole and for endocytosis.

Bruno Saint-Jean, Emilie Seveno-Carpentier, Carine Alcon, Jean-Marc Neuhaus, Nadine P. Paris

The Plant Cell, Vol. 22: 2825–2837, August 2010, www.plantcell.org

The Cytosolic Tail Dipeptide Ile-Met of the Pea Receptor BP80 Is Required for Recycling from the Prevacuole and for Endocytosis [W]

Bruno Saint-Jean,[a] Emilie Seveno-Carpentier,[b] Carine Alcon,[b] Jean-Marc Neuhaus,[c] and Nadine Paris[b,1]

[a] Laboratoire de Physiologie et Biotechnologie des Algues, Institut Français de Recherche pour l'Exploitation de la Mer, 44311 Nantes Cedex 03, France

[b] Biochimie et Physiologie Moléculaire des Plantes, Institut de Biologie Intégrative des Plantes, Unité Mixte de Recherche 5004, Centre National de la Recherche Scientifique/Unité Mixte de Recherche 0386, Institut National de la Recherche Agronomique/ Montpellier SupAgro/Université Montpellier 2, F-34060 Montpellier Cedex 1, France

[c] Laboratoire de Biologie Moléculaire et Cellulaire, Université de Neuchâtel, CH-2009 Neuchâtel, Switzerland

Pea (*Pisum sativum*) BP80 is a vacuolar sorting receptor for soluble proteins and has a cytosolic domain essential for its intracellular trafficking between the *trans*-Golgi network and the prevacuole. Based on mammalian knowledge, we introduced point mutations in the cytosolic region of the receptor and produced chimeras of green fluorescent protein fused to the transmembrane domain of pea BP80 along with the modified cytosolic tails. By analyzing the subcellular location of these chimera, we found that mutating Glu-604, Asp-616, or Glu-620 had mild effects, whereas mutating the Tyr motif partially redistributed the chimera to the plasma membrane. Replacing both Ile-608 and Met-609 by Ala (IMAA) led to a massive redistribution of fluorescence to the vacuole, indicating that recycling is impaired. When the chimera uses the alternative route, the IMAA mutation led to a massive accumulation at the plasma membrane. Using *Arabidopsis thaliana* plants expressing a fluorescent reporter with the full-length sequence of At VSR4, we demonstrated that the receptor undergoes brefeldin A–sensitive endocytosis. We conclude that the receptors use two pathways, one leading directly to the lytic vacuole and the other going via the plasma membrane, and that the Ileu-608 Met-609 motif has a role in the retrieval step in both pathways.

INTRODUCTION

Pea (*Pisum sativum*) BP80 (for binding protein of 80 kD) and its vacuolar sorting receptor (VSR) homologs in *Arabidopsis thaliana* have been extensively studied these last 10 years. BP80 was first identified in clathrin-coated vesicles of developing pea cotyledons by an affinity column using the vacuolar sorting signal from barley (*Hordeum vulgare*) proaleurain as bait (Kirsch et al., 1994). Binding occurred at neutral pH (K_d = 37 nM) with an optimum at pH 6.2 and was abolished at acidic pH. BP80 was shown to be a type I membrane protein with a single transmembrane domain and a cytosolic C-terminal tail of ~5 kD (Kirsch et al., 1994). The cDNA encoding BP80 was later cloned and characterized, and homologs were also identified in *Arabidopsis* (Paris et al., 1997). In parallel, two homologs were identified: At ELP in *Arabidopsis* (Ahmed et al., 1997) and PV72 in precursor-accumulating compartments from developing pumpkin (*Cucurbita* sp cv Kurokawa Amakuri Nankin) seeds (Shimada et al., 1997). In *Arabidopsis*, there are seven BP80 homologs, At VSR1 to At VSR7 (Shimada et al., 2003). Except for At *VSR2* that is expressed only in flowers, the At *VSR*s have largely overlapping expression patterns (Laval et al., 1999, 2003; Neuhaus and Paris, 2006). The function of VSRs as VSRs was confirmed by several independent studies (Humair et al., 2001; Watanabe et al., 2004; Park et al., 2007). It was also shown that At VSR1 (At ELP) and PV72 are involved in the calcium-dependent transport of storage proteins (Shimada et al., 1997; Watanabe et al., 2002; Shimada et al., 2003). It was proposed that At VSR1 serves as a receptor for storage proteins because the *vsr1* knockout mutant accumulates proforms of globulins and albumins and secretes a large amount of storage proteins (Shimada et al., 2003). Nevertheless, At VSR1 does not seem to be the vacuolar receptor for aleurain in seeds because *vsr*1 knockout plants do not missort proaleurain (Shimada et al., 2003). It is still not clear how calcium- and pH-dependent routes interact when the two pathways clearly overlap as in cells of seeds (Oliviusson et al., 2006; Otegui et al., 2006; Craddock et al., 2008).

Electron microscopy studies showed that VSRs are found in prevacuoles and at the *trans*-Golgi network (TGN). In pea root tip cells, BP80 was located in the dilated ends of Golgi cisternae. It was also observed in small structures (roughly the size of a vesicle) associated with the outer periphery of 200-nm translucent compartments that appear to fuse with the large central vacuole (Paris et al., 1997). In *Arabidopsis* roots, VSRs were localized to the *trans* face of the Golgi, most likely the TGN and

[1] Address correspondence to paris@supagro.inra.fr.
The author responsible for distribution of materials integral to the findings presented in this article in accordance with the policy described in the Instructions for Authors (www.plantcell.org) is: Nadine Paris (paris@supagro.inra.fr).

[W] Online version contains Web-only data.

www.plantcell.org/cgi/doi/10.1105/tpc.109.072215

Pep12 compartments (Sanderfoot et al., 1998). VSRs were also found in multivesicular bodies in tobacco (*Nicotiana tabacum*) BY2 cells (Tse et al., 2004) and in *Arabidopsis* seeds (Otegui et al., 2006). The receptors mainly concentrate in the prevacuole rather than in the TGN under native conditions (Paris et al., 1997; Li et al., 2002; Tse et al., 2004). VSRs were found mostly in clathrin-coated vesicles (Kirsch et al., 1994; Hohl et al., 1996; Hinz et al., 2007) but could also be detected in dense vesicles containing storage proteins in seeds (Otegui et al., 2006).

Apart from the specialized seed storage compartments, the accepted model of VSR function proposes that VSRs cycle between the TGN and the prevacuole using shuttle vesicles, in particular clathrin-coated vesicles (Neuhaus and Paris, 2006). Ligand binding most likely occurs in the lumen of the Golgi or in the TGN. Due to progressive pH acidification along the secretory pathway, as demonstrated in mammalian cells (Perret et al., 2005) and supported in plants by the sensitivity of vacuolar transport to V-ATPase inhibitors (Matsuoka et al., 1997), the receptor releases its ligand in the acidic prevacuole. The free receptor is then recycled back to the TGN by a wortmannin-sensitive mechanism (daSilva et al., 2005) that may involve the retromer complex (Oliviusson et al., 2006). Nevertheless, recent data indicate that the retromer could also play a role at the level of the TGN (Niemes et al., 2010b). The released soluble ligands remain in the prevacuolar compartment that most likely matures to a state that is compatible with fusion with the vacuole.

It is believed that multiple cytosolic signals are necessary for receptor trafficking. The Tyr motif is one of the best studied examples of such signals, particularly in mammals. It is composed of a Tyr residue followed by two variable amino acids and a bulky hydrophobic amino acid (YxxΦ). In mammalian cells, the Tyr motifs are involved in clathrin-coated vesicle transport and directly bind to various adaptor proteins depending on their precise sequence (Bonifacino and Traub, 2003, Traub, 2005). Potential Tyr motifs have been found in plant receptors (Geldner and Robatzek, 2008), but their function has so far been demonstrated only in BP80 and in the boron transporter BOR1 where they contribute to the recycling mechanism for the polar localization (Takano et al., 2010). The function of the Tyr motif of At VSR1 (At ELP) was first shown in vitro by a cross-linking binding assay where a peptide derived from At VSR1 was able to compete with mammalian sequences containing a Tyr motif (Sanderfoot et al., 1998). Other in vitro approaches, using pull-down assays and surface plasmon resonance measurements, showed that the pea BP80 Tyr motif binds *Arabidopsis* μA-adaptin, a Golgi-localized protein, with an affinity (K_d) of 144 nM (Happel et al., 2004). Denecke's group studied BP80 trafficking with a nice in vivo competition assay for vacuolar transport (daSilva et al., 2005, 2006) and found that the Tyr motif was necessary for Golgi exit. In its absence, the receptor took an alternative route via the plasma membrane. daSilva et al. (2006) showed the two amino acids Glu-604 and Ile-608 to be involved in receptor trafficking. The in vivo confirmation of the role of the motifs in the context of a full-length receptor prompted us to use a similar approach to further investigate the signals of BP80's cytosolic tail and their role in trafficking.

Based on results in mammalian systems (Bonifacino and Traub, 2003; Ghosh et al., 2003), we chose to analyze further (1) the role of acidic amino acids and (2) the role of Leu-608 and Met-609 (IM dipeptide as part of a dileucine-like motif; EIRAIM). We also further analyzed the role of the Tyr motif YMPL especially in its relation to other cytosolic signals of BP80.

RESULTS

Nine different constructs (Figure 1) with selected amino acid substitutions in the cytosolic tail were made from the original PS1 chimera (a green fluorescent protein (GFP) linked to the transmembrane and cytosolic domains of pea BP80; Kotzer et al., 2004). We transiently expressed these constructs in tobacco epidermal cells and observed their fluorescence pattern. For the original PS1, we found punctate fluorescent structures in the cytosol 72 h after transformation (Figures 2B to 2C). This labeling appeared at the margins in optical sections through the middle of the cell (Figure 2B). In an optical section close to the surface of the cell, spots were easy to visualize (Figure 2B, detailed view). One day earlier, 48 h after transformation, endoplasmic reticulum (ER) labeling was also visible (Figure 2A and inset, ring around the nucleus) and disappeared when the fusion protein had reached its final destination. This labeling is typical for this type of fusion protein and has been extensively described previously (Kotzer et al., 2004; daSilva et al., 2005, 2006). The spots are mostly prevacuolar compartments and sometimes colocalize with Golgi as expected for the TGN (Figure 2F; Li et al., 2002).

To better delineate the distribution of fluorescence, we took z-series of the outer half of the cell and stacked the images to make a three-dimensional projection (Figure 2C). We found that in addition to the dominant punctate pattern, fluorescence could also be detected in the plasma membrane (Figure 2B, arrow) and

```
At VSR3/4  YKYRLRQYMDSEIRAIMAQYMPLDSQPEI/VPNHV/TNDERA
Pea BP80   YKYRIRQYMDSEIRAIMAQYMPLDSQEEG  PNHV  NHQRG
                    |  ⌊⌋  |  |  |
                    E  I  Y  D  E
                    6  M  6  6  6
                    0     1  1  2
                    4     2  6  0
```

PS1					
E604A	X				
IMAA		X			
Y612A			X		
D616A				X	
E620A					X
Y612A + E604A	X		X		
IMAA + Y612A		X	X		
Y612A + D616A			X	X	
Y612A + E620A			X		X

Figure 1. Cytosolic Sequence of BP80 and Mutations Used in This Study.

The cytosolic sequence of pea BP80 and its closest *Arabidopsis* homologs VSR3 and VSR4 were aligned. Amino acids mutated into Ala based on their homology with mammalian signals are shown above the chart. The respective cytosolic domains were fused together with the transmembrane sequence of BP80 to the reporter GFP to produce the unmutated reporter PS1 and mutated reporters E604A, IMAA (I608A plus M609A), Y612A, D616A, and E620A. Numbering of the mutated amino acids was based on the *Arabidopsis* VSR3 sequence.

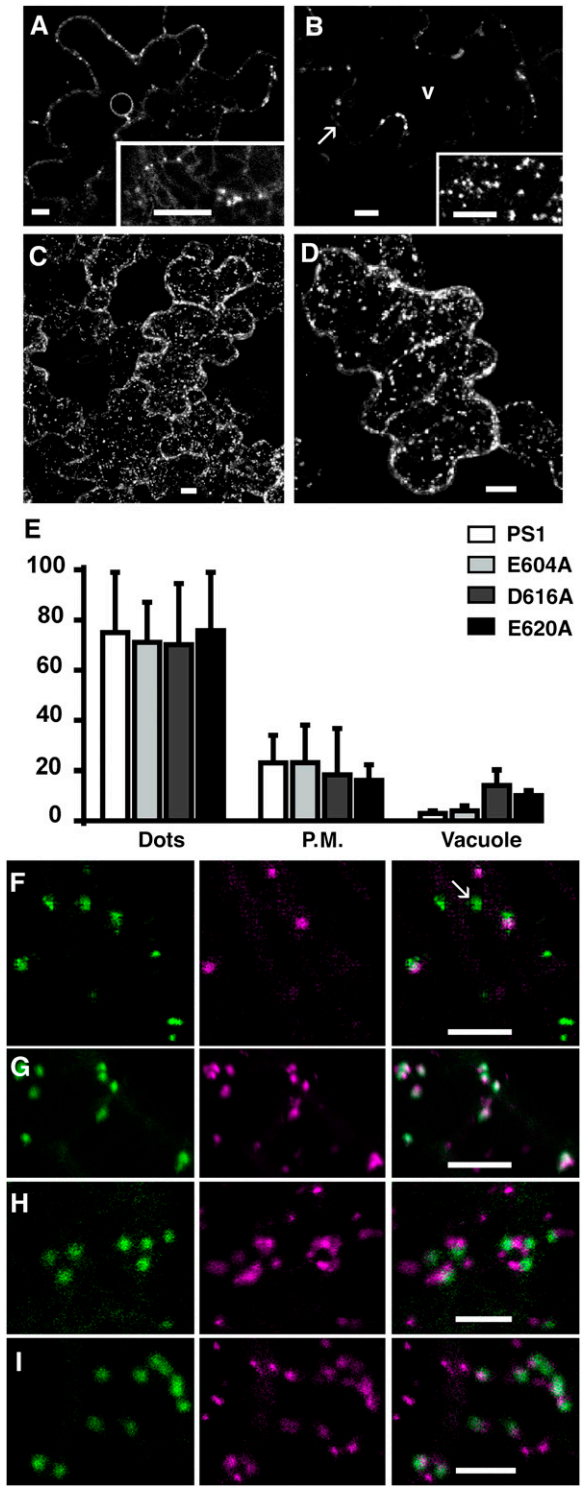

Figure 2. Mutations of Single Acidic Amino Acids Have Minor Effects on the Localization of the Reporter.

Tobacco epidermal cells transiently expressing reporter proteins were observed either 48 **(A)** or 72 h (**[B]** to **[I]**) after transformation. Bars = 10 μm in **(A)** to **(D)** and 5 μm in **(F)** to **(I)**.

(A) The unmutated control reporter PS1 was found in spots and the ER at an early stage of expression as seen in a section through the nucleus and in a section at the surface of the cell (inset).

(B) After 72 h of expression, the reporter has reached its final destination as seen in a section crossing through the vacuole (v) at the level of the nucleus with little labeling at the plasma membrane (arrow). Typical punctate structures can be better visualized in an optical section through the cytosol (inset).

(C) Accumulation of individual z-sections of cells expressing PS1 reporter.

(D) Accumulation of individual z-sections from a cell expressing E604A mutated reporter.

(E) Relative fluorescence intensity in three chosen locations, dots, plasma membrane (P.M.), and vacuole for the following constructs: control PS1 (white), E604A (light gray), D616A (dark gray), and E620A (black). Error bar stands for SD from 90 to 150 measures for each subcellular location and each construct.

(F) to **(I)** Tobacco epidermal cells transiently coexpressing PS1-based reporter proteins (green) and the Golgi reference ERD2-CFP (purple). The reporter protein was either PS1 **(F)**, E604A **(G)**, D616A **(H)**, or E620A **(I)**. **(F)** Typical prevacuole labeling (arrow) is separated from Golgi labeling.

inside the vacuole (Figure 2B, v) but with intensity that slightly varied between cells and expression experiments. We therefore quantified in z-stacks the average fluorescence intensity in each of the three subcellular locations: punctate structures, plasma membrane, and vacuole (see Methods for more details). This quantification was made on at least 90 independent measurements for each of the three subcellular locations. The average signal intensity obtained for each subcellular location was then expressed relative to the total fluorescence (punctate structures plus plasma membrane plus vacuole representing 100%). The quantification shown in Figure 2E for PS1 confirmed that fluorescence is mostly (almost 80%) in dots. To make sure that this distribution reflects the final destination of the chimera, we also quantified fluorescence of stably transformed tobacco plants expressing the PS1 construct (see Supplemental Figure 1 online). Indeed, in these plants, the fluorescence was 84% in dots, 14.5% in plasma membrane, and 1.5% in vacuole

Mutations of Acidic Amino Acids Have Mild Effects

We first expressed chimeras with mutations in each of three acidic amino acids found in the cytosolic tail of BP80. Glu-604 is conserved in all 23 plant homologs identified so far. Asp-616 is conserved in pea and all *Arabidopsis* homologs, while Glu-620 is found in pea BP80 and its two closest *Arabidopsis* homologs, At VSR3 and At VSR4. As shown for E604A in a z-stack projection (Figure 2D), the labeling pattern for all three mutants was similar to the pattern for the PS1 control. Quantitative intensity measurement confirmed there was no significant difference in distribution, except for a fluorescence increase in the vacuole compared with the control (4 times for D616A and 3 times for E620A; Figure 2E). To find out if these mutations modified protein partitioning between the Golgi/TGN and the prevacuole, we coexpressed each of the three mutants with the Golgi marker ERD2-CFP (for cyan fluorescent protein). As expected, the PS1 construct accumulated mainly in prevacuolar compartments distinct from the Golgi (Figure 2F, arrow). The same was true

for the two mutants D616A and E620A (Figures 2H and 2I, respectively). By contrast, distribution of the E604A mutant protein clearly differed from that of PS1; it colocalized almost exclusively with the Golgi marker (Figure 2G). To conclude, mutating the acidic amino acids had mild effects on the reporter's distribution. Mutating Glu-604 increased Golgi localization, whereas mutating Asp-616 and Glu-620 only slightly increased exposure of the fusion protein to a lytic environment.

Mutation of the Tyr Motif Leads to a Partial Redistribution of the Reporter to the Plasma Membrane

To test the role of the Tyr motif on the subcellular localization of the reporter, we transiently expressed the mutated chimera Y612A (Figure 1) in tobacco epidermal cells. As shown by a three-dimensional reconstruction of labeled cells, the distribution of the reporter appeared very similar to the distribution of PS1 except that the plasma membrane seemed more fluorescent than in the control (cf. Figures 3A and 2C). To confirm this observation, we quantified fluorescence intensity in the three subcellular locations: punctate structures, plasma membrane, and vacuole. There was indeed almost twice as much fluorescence in the plasma membrane compared with the control, with no change in the vacuole (Figure 3C).

Mutating Both Ile-608 and Met-609 Leads to a Massive Redistribution of the Reporter to the Vacuole

To test the role of the IM dipeptide, we expressed the IMAA chimera, in which both Ile-608 and Met-609 were mutated to Ala (Figure 1). We analyzed the subcellular localization of the fluorescence after 72 h of expression. As shown on Figure 3B, the distribution of fluorescence was drastically different from that of PS1; the vacuole appeared strongly labeled (Figure 3B, v). The nucleus is visible in negative contrast (Figure 3B, arrow). Quantitatively, the IMAA vacuolar fluorescence was 25 times higher than for PS1 (Figure 3C). Fluorescence inside the vacuole can be explained by cleavage and release of the soluble reporter from the membrane-bound fusion protein. We noticed that the vacuolar labeling gradually appeared during the transient expression and peaked at 64 to 72 h after transformation. After only 48 h of transient expression, fluorescence was found in small dots (Figures 3D and 3E) and then decreased concomitantly with the appearance of vacuolar staining.

To gain further insights into the nature of these intermediate compartments, we coexpressed the IMAA construct with the Golgi reference ERD2-CFP and observed doubly transformed cells 48 h after transformation, when punctate labeling was dominant. As shown in Figure 3F, the compartments labeled with IMAA were almost entirely distinct from the Golgi. We then coexpressed the soluble reporter cargo Aleu-CFP that is transported to the vacuole by VSRs. This reporter contains the vacuolar sorting signal of petunia (*Petunia hybrida*) aleurain that is sufficient for vacuolar targeting (Humair et al., 2001). When expressed in plants, this soluble cargo reporter was also found first in small dots that are believed to be prevacuolar intermediates prior to vacuole delivery (Flückiger et al., 2003; Kotzer et al., 2004). When Aleu-CFP was coexpressed with IMAA and cells were observed 48 h after transformation, IMAA and Aleu-CFP spots were found to totally colocalize (Figure 3G), indicating the prevacuolar nature of IMAA intermediate compartments. Altogether, this indicates that mutating the IM dipeptide strongly affects the reporter distribution, decreasing Golgi localization in favor of prevacuolar localization. Prevacuolar fluorescence is transient, indicating that recycling of the reporter is impaired.

In Contrast with Asp-616 and Glu-620, Mutating Glu-604 Has Some Effect Even in Absence of the Tyr Motif

We tested the role of the Tyr motif in relation to the three acidic amino acids by generating double mutants and then transiently expressing them in tobacco epidermal cells. The double mutants had a pattern of expression that resembled the nonmutated control PS1 (Figures 4B to 4E). Quantification revealed that plasma membrane fluorescence intensity for all three mutants was actually closer to Y612A (Figure 4A) than to PS1 (Figure 3C). In contrast with the single mutants D616A and E620A, fluorescence intensity in the vacuole did not increase for the corresponding double mutants (Figure 4A vacuole compared with Figure 2E vacuole). This indicates that the Tyr mutation is dominant and masks the effect of the Asp-616 and Glu-620 mutations. We then addressed the nature of the dots by coexpression with a Golgi reference marker and found that the Glu-604 mutation caused a redistribution of the marker to the Golgi/TGN (Figure 4C), as was already observed with the single mutant (Figure 2G). Because the Tyr motif mutation is redirecting receptor trafficking to an alternative pathway, this indicates that Asp-616 and Glu-620 function only in the main pathway, whereas Glu-604 is likely to play a role in both pathways.

The IM Dipeptide Is Also Involved in Endocytosis

To address the relative roles of the Tyr and the IM motifs, we prepared a corresponding double mutant (Figure 1). We transiently expressed the IMAA+Y612A construct in tobacco epidermal cells. The mutant protein showed a major localization at the plasma membrane with very few intracellular dots (Figure 4F). Quantification of signal intensity clearly confirmed redistribution of this mutant to the plasma membrane (Figure 4I). The signal intensity in the plasma membrane was 3 times higher than that for PS1. To ensure that the whole reporter reached the plasma membrane, we plasmolysed transformed cells and found that labeling remained associated with the plasma membrane (Figures 4G and 4H, arrow with a star), whereas the extracellular space was unstained. This confirmed that the fluorescence was due to the membrane-bound reporter and not to a released and secreted core GFP. The fluorescence intensity at the plasma membrane almost doubled for IMAA+Y612A in comparison to Y612A alone (Figure 4I), indicating that the IMAA motif is important for endocytosis. Additionally, very few spots could also be detected for the IMAA+Y612A reporter. We identified these as being mostly Golgi or closely associated with it since they colocalized with ERD2-GFP (Figure 4J). The fact that we found very little fluorescence in the vacuole for IMAA+Y612A (in contrast with the IMAA mutant) indicates that the Tyr-612 mutation

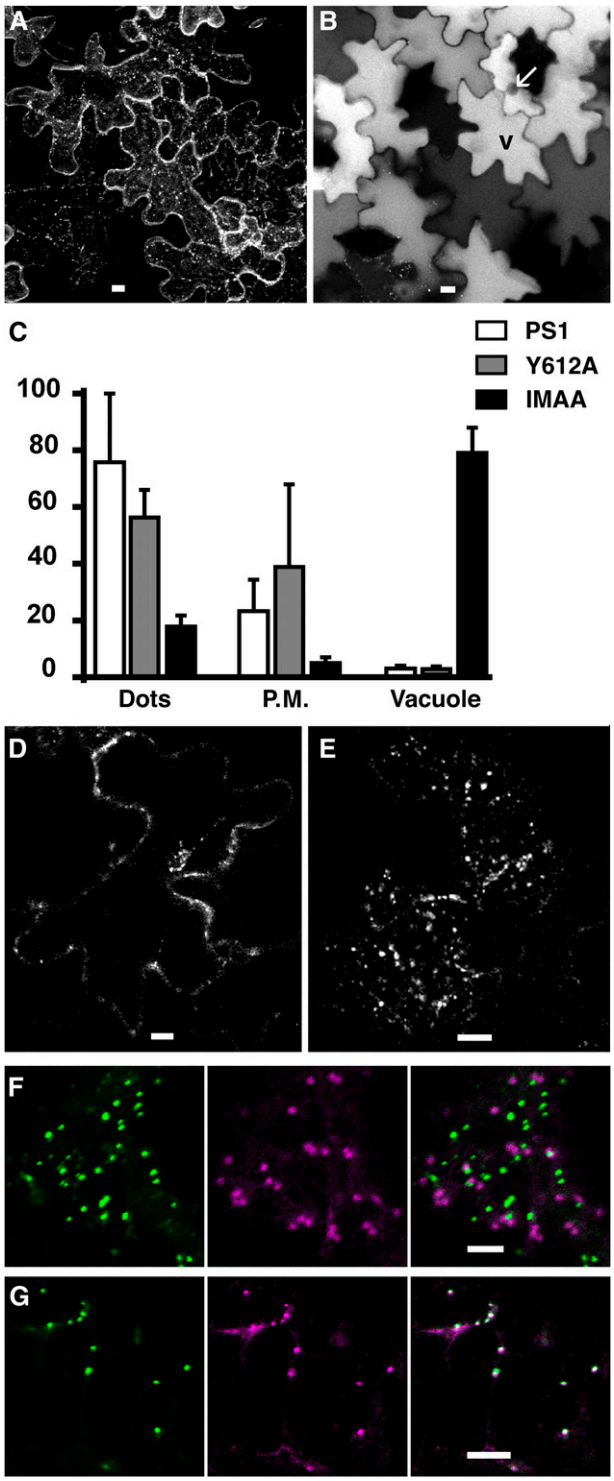

Figure 3. The Y612A Mutation Increases the Presence of the Reporter at the Plasma Membrane, While the IMAA Mutation Leads to GFP Accumulation in the Vacuole.

Tobacco epidermal cells transiently expressing reporter proteins were observed either 72 (**[A]** to **[C]**) or 48 h (**[D]** to **[G]**) after transformation using a confocal microscope. Bars = 10 μm in **(A)**, **(B)**, **(D)**, and **(E)** and 5 μm in **(F)** and **(G)**.

(A) Accumulation of individual z-sections from cells expressing Y612A.

(B) A single section of cells expressing the IMAA reporter shows a massive fluorescence accumulation in the vacuole (v) leading to a negative staining of the nucleus (arrow).

(C) Relative fluorescence intensity in three chosen locations, dots, plasma membrane (P.M.), and vacuole, for the following constructs: control PS1 (white), Y612A (gray), and IMAA (black). Error bar stands for SD from 90 to 150 measures for each subcellular location and each construct.

(D) and **(E)** Single sections at the level of the nucleus **(D)** or at the surface **(E)** for cells expressing IMAA show intermediate labeling of spots prior to vacuole accumulation.

(F) and **(G)** Coexpression of IMAA (green) either with a Golgi reference ERD2-CFP (**[F]**; purple) or with the BP80 ligand Aleu-CFP (**[G]**; purple).

dominates over the retrieval effect of IMAA, perhaps by preventing the fusion protein from reaching prevacuolar compartments.

The Full-Length Receptor Is Also Partially Localized to the Plasma Membrane

To find out if the luminal domain of VSRs could have an influence on the plasma membrane localization of the reporter, we made a fusion protein of the citrine fluorescent protein and the full-length receptor. We positioned the fluorescent reporter between the signal peptide and the rest of the coding sequence of the *Arabidopsis* homolog At *VSR4* (the closest homolog of pea BP80). This chimera should be functional because a similar construct was able to bind its ligand aleurain in vivo as shown by bimolecular fluorescence complementation (Park et al., 2007). The fusion citrine-*AtVSR*4 was transiently expressed in tobacco epidermal cells, and its distribution was observed after 72 h of expression. As shown in Figure 5, citrine-AtVSR4 accumulated in dots (Figure 5A) and also in the plasma membrane (Figure 5B) but not in the ER (Figure 5C, n indicates the nucleus). The partitioning of fluorescence among the dots, the plasma membrane, and the vacuole was similar to what was found for the PS1 fusion protein. Indeed, the fluorescence intensity in the plasma membrane reached ~30% while it represented roughly 20% without the luminal domain of the receptor (Figure 2E, PS1). We then addressed the nature of the dots by coexpressing citrine-*AtVSR*4 with a CFP version of PS1. As shown in Figure 5D, both fusion proteins colocalized. This result indicates that a potentially functional receptor can also be found in the plasma membrane.

We next transformed *Arabidopsis* plants with the citrine-*AtVSR*4 chimera. We obtained six fluorescent lines that all presented a dominant spot-like labeling as shown in the root apex (Figure 5E). In addition, we observed in all plants additional labeling of the plasma membrane. This plasma membrane labeling was not detectable in root apex cells but increased gradually along the root's longitudinal axis to be clearly visible in the medium part of the root (Figure 5F) and was dominant in the upper part of the root (Figure 5G). In two plants out of six, we could barely detect any dot labeling in cells from the upper region of the root (plants G and H). Since citrine-*AtVSR*4 is expressed

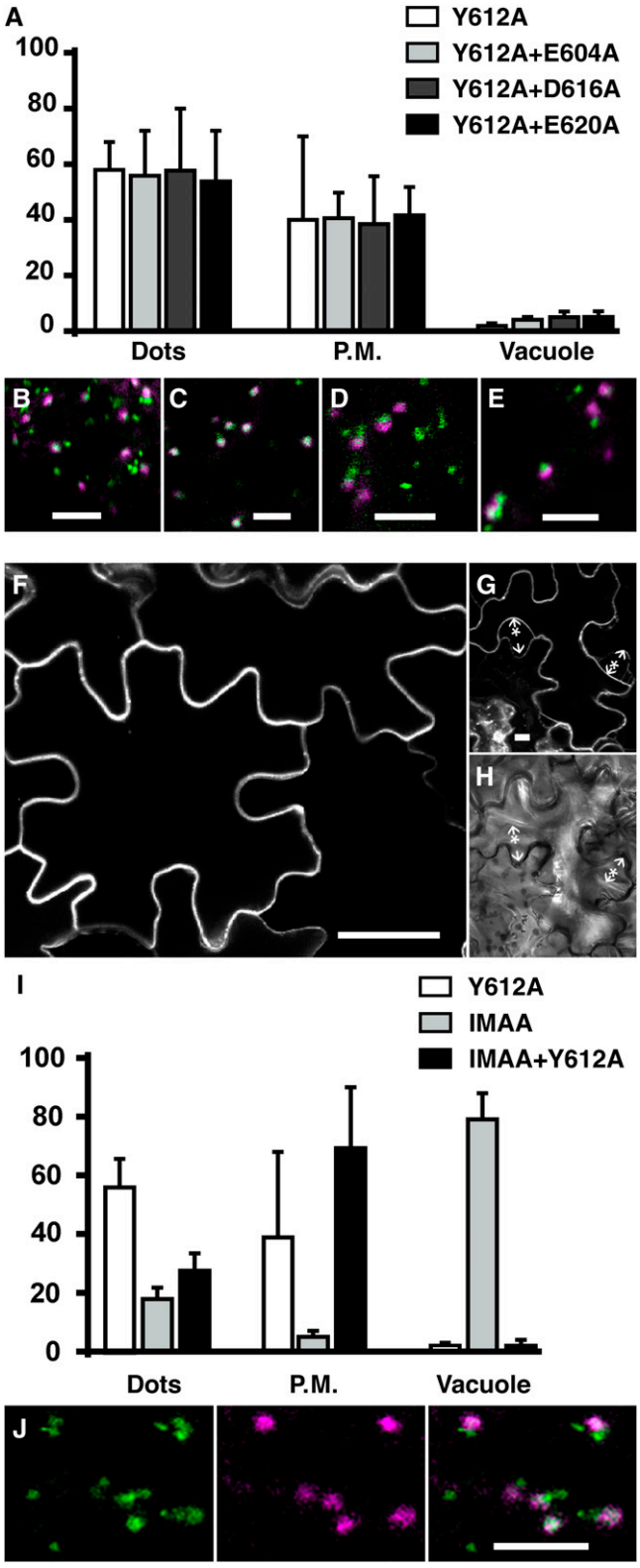

Figure 4. In the Absence of a Functional Tyr Motif, the IMAA Mutation Blocks the Reporter in the Plasma Membrane, While Mutating Acidic Amino Acids Have Minor Effects.

using a 35S promoter, as a control we determined by immunoblotting the level of protein in comparison to the native receptor. We found similar quantities of the fusion and the native proteins (see Supplemental Figure 2 online), indicating that the fluorescent chimera is not massively overexpressed.

The Receptor Undergoes Endocytic Recycling at the Plasma Membrane

We took advantage of the exclusive plasma localization of citrine-AtVSR4 in the upper root cells to examine the dynamics of its endocytosis and exocytosis. We applied brefeldin A (BFA), a fungal metabolite used to inhibit vesicular trafficking at the exocytosis/secretion level, in presence of the protein biosynthesis inhibitor cycloheximide. In *Arabidopsis* root cells, BFA treatment leads to the intracellular accumulation of endocytic material in so-called BFA compartments. Plasma membrane proteins that undergo BFA-sensitive endocytic recycling accumulate in these compartments. Since BFA experiments are usually performed with cells close to the root apex, we performed a control experiment on the upper root cells expressing the plasma membrane fusion protein LTi6a-GFP (Cutler et al., 2000). As shown on Figure 6B, upper root cells form typical LTi6a-GFP–containing BFA compartments after BFA treatment as described in apex cells (Dhonukshe et al., 2007).

We therefore performed the same treatment on citrine-At*VSR4*–expressing roots and found a clear accumulation of fluorescence in BFA bodies (Figure 6A). Interestingly, while an important fraction of LTi6a-GFP remained at the plasma membrane after BFA treatment, we observed a strong decrease to full disappearance of plasma membrane labeling for citrine-AtVSR4 (Figure 6A, arrow). Since cycloheximide is depleting the cells in newly synthesized proteins, we controlled that labeling of citrine-AtVSR4 was stable along the duration of the experiment by treatment with cycloheximide alone (Figure 6C). The accumulation of citrine-AtVSR4 in BFA compartments together with a

Tobacco epidermal cells expressing transiently reporter proteins were observed 72 h after transformation using a confocal microscope. In **(A)** and **(I)**, error bar stands for SD from 90 to 150 measures for each subcellular location and each construct. Arrow, cell wall; arrow with a star, plasma membrane. Bars = 5 μm in **(B)** to **(E)** and **(J)** and 10 μm in **(F)** and **(G)**.

(A) Relative fluorescence intensity in three chosen locations, dots, plasma membrane (P.M.), and vacuole, for the following constructs: Y612A (white), Y612A+E604A (light gray), Y612A+D616A (dark gray), and Y612A+E620A (black).

(B) to **(E)** Coexpression of the reporter proteins Y612A (**[B]**; green), Y612A+E604A (**[C]**; green), Y612A+D616A (**[D]**; green), or Y612A+E620A (**[E]**; green) with the Golgi reference ERD2-CFP (purple).

(F) to **(H)** Single confocal section of epidermal cells taken at the level of the nucleus, under normal conditions **(F)** or after plasmolysis (**[G]** and **[H]**).

(I) Relative fluorescence intensity in three chosen locations, dots, plasma membrane (P.M.), and vacuole, for the following constructs: Y612A (white), IMAA (gray), and IMAA+Y612A (black).

(J) Coexpression of IMAA+Y612A (green) with a Golgi reference ERD2-CFP (purple).

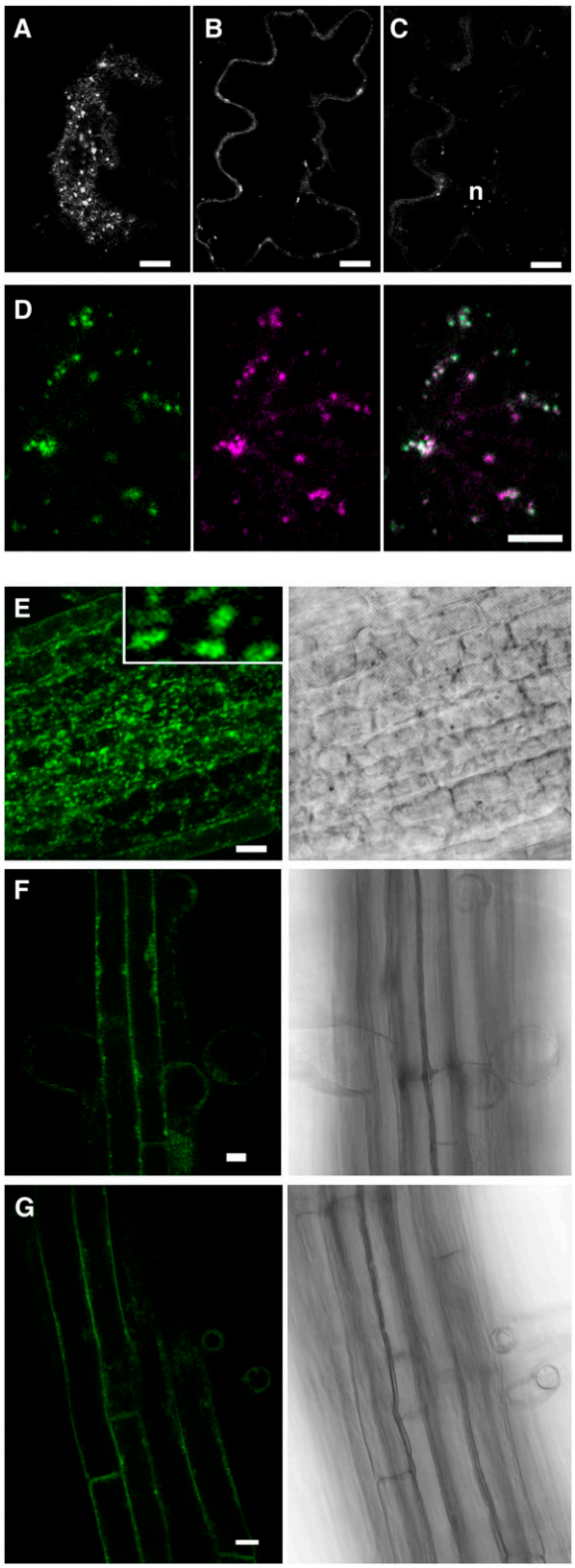

Figure 5. A Full-Length VSR Fused to a Fluorescent Protein Partially Localizes in the Plasma Membrane and Colocalizes with the PS1 Reporter

decrease of plasma membrane labeling indicates that the receptor undergoes endocytosis. In contrast with the LTi6a-GFP control, we also observed a faster accumulation of citrine-AtVSR4 in BFA compartments (10 min of BFA treatment compared with 60 min for Lti6a-GFP).

We next tested the ability of the receptor to participate in exocytosis by washing off the BFA in presence of cycloheximide. As shown on Figures 6D and 6E, BFA compartments visible before washing (Figure 6D) disappeared after removal of BFA, while plasma membrane labeling was recovered (Figure 6E). This indicates that the receptor can traffic from internal compartments to the plasma membrane. In conclusion, plasma membrane–localized citrine-AtVSR4 undergoes BFA-sensitive exo- and endocytic cycling.

DISCUSSION

VSR Trafficking and Signals

The main result of this study is the identification and characterization of a novel signal, the dipeptide IM that is conserved in all the VSRs identified so far. IM is involved in two trafficking steps: (1) the recycling from the prevacuolar compartment and (2) endocytosis. Based on our results, and on previous observations of daSilva et al. (2006), we propose the following model (Figure 7) with a main pathway (green and blue arrows) and an alternative pathway (orange arrows). In the main pathway, the receptor recognizes its ligand in the TGN, releases it into the prevacuole, and recycles back to the TGN. The contention that acidification is a necessary component for vacuolar transport is supported (1) by in situ pH measurements in mammalian cells giving values of 6.2 in the TGN and <5.5 in the prelysosomal compartment (Anderson and Orci, 1988; Miesenböck et al., 1998), (2) by the fact that V-ATPase inhibitors disrupt the transport of vacuolar soluble cargo in plants (Matsuoka et al., 1997), and (3) by pH-dependent binding of pea BP80 to its ligands (Kirsch et al., 1994). As previously suggested (daSilva et al., 2006), we found that the Tyr motif is used for the exit step from the TGN to the prevacuole/multivesicular body (MVB) (Figure 7, step 1 and green arrows). The observed increase in vacuolar accumulation of released core GFP argues for a major role of the

(A) to **(D)** Tobacco epidermal cells transiently expressing reporter proteins were observed 72 h after transformation using a confocal microscope.

(A) to **(C)** Confocal sections of an epidermal cell expressing citrine-*AtVSR4* taken either at the surface **(A)**, deeper inside the cell **(B)**, or at the level of the nucleus **(C)**.

(D) Coexpression of PS1 fused to CFP (green) with citrine-*AtVSR4* (purple).

(E) to **(G)** *Arabidopsis* plantlets stably expressing citrine-*AtVSR4*. Roots from 7-d-old plants were observed with a confocal microscope with the bright-field setting (right side) or under fluorescence confocal mode (left side) at different levels: the apex (**[E]** and inset: 10 times enlarged detail), the middle portion **(F)**, or the top part **(G)**.

n, nucleus. Bars = 10 μm.

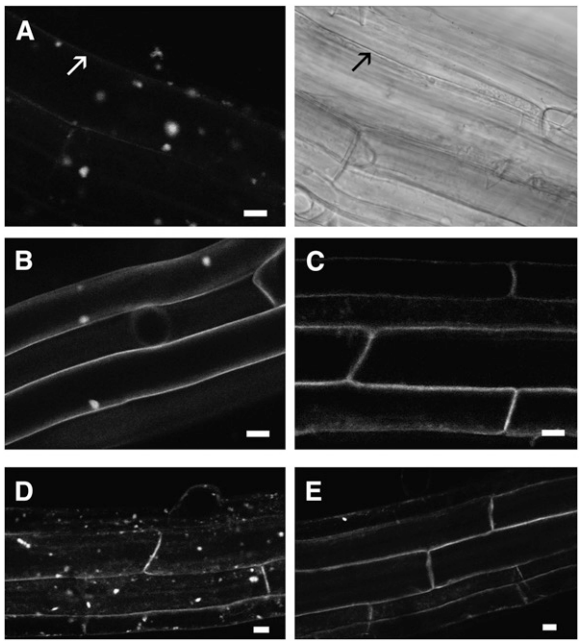

Figure 6. Citrine-AtVSR4 Undergoes BFA-Sensitive Endocytic Recycling

One-week-old plants expressing citrine-*AtVSR4* were submitted to BFA treatment (50 μM) for 60 min in presence of 50 μM cycloheximide. Cells from the top portion of the root, where the fusion protein is exclusively found in the plasma membrane, were observed using a confocal microscope. Arrow, plasma membrane. Bars = 10 μm.
(A) Citrine-AtVSR4 labeling after BFA treatment. The right side shows a bright-field image of the same cells shown on the left.
(B) Control plants expressing LTi6a-GFP after BFA treatment.
(C) Citrine-AtVSR4 after 60 min of cycloheximide treatment. Plasma membrane labeling of citrine-AtVSR4 had fully recovered after BFA treatment for 10 min **(D)** and a subsequent wash in cycloheximide for 80 min **(E)**.

IM dipeptide and for a minor role of Asp-616 and Glu-620 in the retrieval step (Figure 7, step 3 and blue arrows). The requirement of the cytosolic domain and in particular of a functional Tyr motif to efficiently reach the post-Golgi lytic compartments is also supported by the Golgi accumulation of a fusion protein lacking the whole cytosolic domain of VSR (Brandizzi et al., 2002).

The alternative pathway involves the TGN/early endosome and the plasma membrane (black and orange arrows, Figure 7). In the absence of a functional Tyr motif, the receptor is forced to take this alternative route (Figure 7, step 5), as indicated by an increase of plasma membrane labeling. The remaining presence of internal labeling when the Y612A construct was used indicates either that the transport from the TGN to plasma membrane is not very efficient or that internalization of the receptor counterbalances the effect of mutating Tyr. We found that mutating the IM dipeptide in addition to Tyr doubles the fluorescence intensity at the plasma membrane, inverting the proportions of dots and plasma membrane in comparison to a nonmutated receptor. This clearly indicates that IM is involved in this endocytosis step (Figure 7, step 7 and orange arrows). We cannot exclude the possibility that the Tyr motif is involved as well in endocytosis since Y612A is also partially accumulated in the plasma membrane.

Surprisingly, we found no increase of vacuolar labeling when mutating IMAA and Y612A together. We therefore propose that the alternative pathway does not include compartments that reside further down the early endosome on the vacuole route. Instead, we propose that the Y612A mutant cycles between the plasma membrane and the early endosome (EE). We confirmed

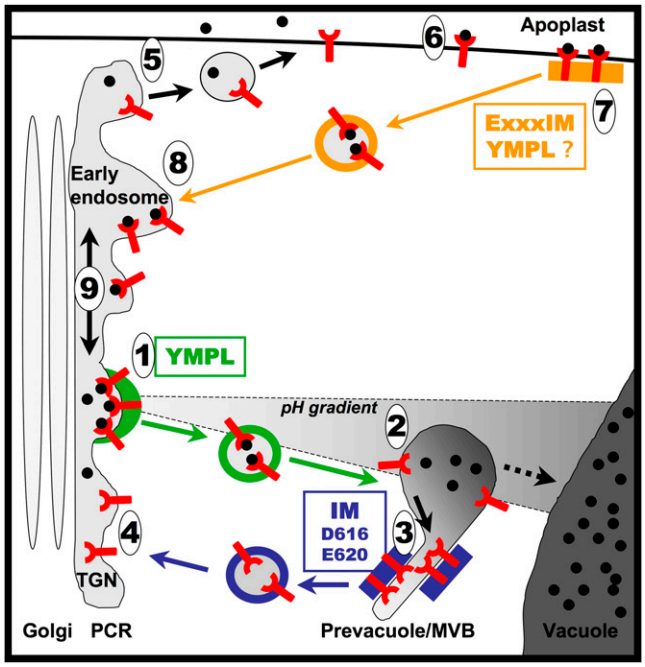

Figure 7. Proposed Trafficking Model for the VSR BP80.

The receptor BP80 uses a major (green and blue arrows) or an alternative pathway (black and orange arrows). In the major pathway, BP80 recognizes the ligand (black circle) at the level of the TGN that is part of a PCR. The exit from the TGN (1) requires the YMPL motif most likely through its interaction with μA-adaptin containing complex (green box and vesicle coat). After fusion of the vesicle to the prevacuole (2), the receptor releases its ligand, possibly due to a pH decrease. The free receptor is then segregated out of the ligand release area (3) most likely by interaction of the IM motif with a retrieval complex (blue box). The free receptor is packed in coated vesicles (vesicle with blue coat) back to the TGN where fusion (4) may require VPS45. The final steps for ligand transport to the vacuole (dashed arrow) do not require BP80 but instead are believed to be maturation processes of the prevacuole/MVB that eventually fuses with the vacuole. The alternative pathway serves to retrieve missorted ligands from the apoplast. The free receptor but also free ligand can exit the PCR (5; black arrows) to reach the plasma membrane by a BFA-sensitive process. At the plasma membrane, the receptor binds a ligand (6) and is endocytosed using the IM dipeptide as part of a dileucine-like motif ExxxIM possibly with the help of the Tyr motif. The endocytosis signal should interact (7) with the retrieval complex (orange box and vesicle coat). Fusion of the vesicle with the early endosome (8) leads to release the receptor-ligand complex in the PCR where the complex can diffuse along the membrane (9) and may enter the main pathway thanks to the Tyr motif (1).

that the receptor undergoes a BFA-sensitive endocytic cycling in *Arabidopsis* transgenic plants expressing a fusion protein with the entire sequence of At VSR4 at a level similar to the endogenous form. The plant apoplastic environment is compatible with ligand recognition since the optimal pH for VSR binding is ~6.2 (Kirsch et al., 1994), while the extracellular pH is close to 6 (Grignon and Sentenac, 1991; Gao et al., 2004). Therefore, the plasma membrane-EE pathway identified in our expression and mutation assays is not a default pathway due to overexpression, but an alternative pathway, most likely used to retrieve ligands that escaped the sorting step at the TGN, like the mammalian mannose-6-phosphate receptors (MPR) do for escaped lysosomal proteins (Ghosh et al., 2003). The fact that VSRs were also identified in a purified plasma membrane fraction (Laval et al., 1999) also supports this conclusion.

Two publications show that the TGN, labeled by the secretory carrier membrane protein 1 and the V-ATPase subunit VHA1, is the first intracellular station of endocytosed cargoes before going to MVBs (Dettmer et al., 2006; Lam et al., 2007). These two publications indicate that in plants the TGN, defined by electron microscopy as a Golgi-associated partially clathrin-coated reticulum (PCR), may also function as an EE. It is likely that the EE and the TGN may represent subdomains of a same PCR compartment. The receptor could move from EE to the TGN and use either one of the two pathways (Figure 7, step 9).

We also addressed the role of acidic residues in the cytosolic tail and found that their mutations had minor effects on VSR trafficking. Glu-604 may participate either in some early transport step prior to the splitting point between the two pathways, while Asp-616 and Glu-620 may participate in recycling from the prevacuole (Figure 7, step 3). This is in accordance with daSilva's results (daSilva et al., 2006) where E604A caused a strong loss in the competitive effect of the mutated receptor, without changing core-GFP release.

VSR Trafficking Partners

VSRs are so far the only examples of plant receptors with a demonstrated trafficking signal using clathrin-coated vesicles. The mechanism of clathrin coat assembly at Golgi and plasma membrane is well described in mammalian cells (Traub, 2005). The coat is composed of an inner layer of adaptors and an outer layer of clathrin. Adaptors play a key role by interacting with both the membrane cargo (or receptors) and the clathrin. Cargo incorporation into the complex is highly regulated and implicates four classes of signals carried by the cargo proteins or receptors: the Tyr motif (YxxØ), the acidic cluster-dileucine signal (DxxLL), the dileucine signal ([D/E]xxxL[L/I/M]), and the Tyr-based motif (FxNPxY). All plant VSRs identified so far contain a conserved Tyr motif (YMPL). The *Arabidopsis* μA-adaptin was shown to bind to the Tyr motif of VSRs, presumably at the level of the TGN (Ahmed et al., 2000; Happel et al., 2004). EpsinR1, a phosphoinositide and clathrin binding protein, was also shown to participate in the vacuolar transport of soluble cargo (Song et al., 2006), while the related EpsinR2 seems to participate in a different pathway (Lee et al., 2007).

Retrograde transport of VSRs was shown to depend on the retromer complex (Oliviusson et al., 2006; Shimada et al., 2006; Niemes et al., 2010a, 2010b). No motif for retromer-mediated sorting has yet been identified in the cytosolic tail of plant receptors, but our data indicate that the IM dipeptide could be a good candidate.

Endocytosis and a Putative Dileucine Motif

Endocytosis was long considered impossible in plants because turgor pressure would prevent membrane invagination. It is now clear from numerous independent studies that endocytosis can occur, even in guard cells. With the help of fluorescent proteins and drugs such as wortmannin and BFA, our knowledge of endosomal compartments has greatly progressed as reviewed recently (Geldner and Robatzek, 2008; Robinson et al., 2008). In plants, a role of a Tyr motif in endocytosis is supported by the fact the human transferrin receptor appears to be functional for endocytosis in plant cells (Ortiz-Zapater et al., 2006). Recently, a Tyr motif was found to be implicated in the endocytosis-mediated polar localization of *Arabidopsis* BOR1 (Takano et al., 2010). When cryptogein, a molecule derived from an oomycete, was applied to BY2 tobacco cells, it enhanced the uptake of the lipophilic reagent FM4-64, a classical marker for endocytosis. The number of clathrin-coated pits was also found to increase upon cryptogein treatment, and tyrphostin A23 had an antagonistic effect on cryptogein-induced endocytosis (Leborgne-Castel et al., 2008).

In the case of VSRs, Tyr-612 has been shown to be part of a Tyr motif, and its binding to a Golgi-localized μA adaptin supports a function in the TGN exit step (Happel et al., 2004). This nevertheless does not exclude a function in endocytosis where the dipeptide IM clearly plays a role. The context of the IM dipeptide in VSRs, ExxxIM, resembles the canonic sequence of a dileucine signal [D/E]xxxL[L/I/M]. In mammalian cells, such signals have been identified as endocytosis signals in several membrane proteins, including CD3 γ-chain and MPRs. This motif binds to the μ subunit of AP1, 2, and 3. The ExxxIM in VSRs could be such an endocytic dileucine-like motif. In mammalian cells, the acidic residue appears to be important for targeting to later endosomal compartments but not for the internalization itself (Pond et al., 1995; Sandoval et al., 2000). This fits with our observation that the Glu-604 mutation did not affect endocytosis in the Y612A mutant.

The IM Motif Contributes to Two Pathways

The IM motif found in VSRs clearly plays a dual role in receptor trafficking. There is at least one example of a similar motif in a mammalian receptor that also plays a dual role in trafficking. Like VSRs, the cation-independent MPR (CI-MPR) is involved in transporting lytic enzymes and is present in the TGN, the early endosomes, the recycling endosomes, and the plasma membrane (Ghosh et al., 2003). Its cytosolic domain contains numerous trafficking signals, including a Tyr motif (YSKV) and the tripeptide WLM, which has a dual function. Mutation of the WLM motif led to a massive degradation of the reporter fusion protein CD8-CI-MPR, therefore demonstrating its role in recycling (Seaman, 2007). This tripeptide was also required for binding to retromer proteins. These features are shared with a similar tripeptide FLV in sortilin, leading to the conclusion that [W/F]L[M/V] is a

consensus motif for retromer-mediated retrieval from endosomes to TGN in mammals (Seaman, 2007). Interestingly, WLM in CI-MPR is also part of an unconventional dileucine motif ETEWLM that binds the γ and σ subunits from the adaptator complex AP1 (Traub, 2005) but also favors binding of the Tyr motif to the μ subunit of the same AP1 complex (Lee et al., 2008). In support of these results, Seaman found that neither AP1 nor retromer could be coimmunoprecipitated with CI-MPR when WLM was mutated, but he also demonstrated that the retromer and the AP1 complexes mediate two distinct pathways. Therefore, the tripeptide WLM of CI-MPR is both a retrieval signal for the retromer and a dileucine-like signal for the AP1-mediated transport in cooperation with the Tyr motif. In VSRs, the IM motif could correspond to the retromer association signal [W/F]L[M/V], although the preceding amino acid is never aromatic in any VSR identified so far but is instead almost always an Ala and rarely a Ser or a Thr.

In our model, the same IM motif is used in two different trafficking steps of VSR trafficking, but in the main pathway, the receptor is ligand-free, while it would be bound in the alternative route. In some mammalian receptors, dileucine signals are modulated by Ser phosphorylation (Pitcher et al., 1999; von Essen et al., 2002). Interestingly, the dileucine-like signal of VSRs is also preceded by a Ser (SExxxIM), which has a good probability of in vitro phosphorylation (Blom et al., 1999).

METHODS

Constructs

The coding sequence for GFP-PS1 was described previously (Kotzer et al., 2004) and contains the GFP reporter followed by the transmembrane and the cytosolic domains of pea (*Pisum sativum*) BP80 (Paris et al., 1997). We used the previously described GFP6 (Di Sansebastiano et al., 2001) with the double mutation F64L and S65T (Cormack et al., 1996).

A *Sal*I site was created at the fusion between the *GFP* and *BP80* coding sequences with no change in either one of the two protein sequences, and a *Sac*I site was added at the level of the stop codon. The resulting coding sequence at the fusion is MDELYKSTW*AAF* where the underlined K, preceding the transmembrane domain (italic), is shared by GFP and BP80 sequences. Point mutations, changing chosen amino acids to Ala, were introduced in the cytosolic sequence of BP80 by overlapping PCR. The resulting PCR fragments were verified by sequencing and used to substitute the original sequence using *Sal*I and *Sac*I sites. This generated nine new constructs coding for proteins with one, two, or three altered amino acids. The constructs were named according to the point mutations introduced at the level of the cytosolic domain of pea BP80: E604A, IMAA (I608A+M609A), Y612A, D616A, E620A, Y612A+E604A, IMAA +Y612A Y612A+D616A, and Y612A+E620A. For easier comparison with published data (daSilva et al., 2006), these numbers correspond to the positions of targeted amino acids in reference to the sequence of the *Arabidopsis thaliana* homolog *VSR3*. All constructs were finally transferred into the binary vector pVKH18En6 for transient expression under the control of the strong 35S promoter (Batoko et al., 2000).

A fusion of the citrine sequence (Griesbeck et al., 2001) with the full-length sequence of *Arabidopsis VSR4* was made by inserting the reporter between the signal peptide and the sequence of the mature At *VSR4* by creating a *Pst*I in 5′ and a *Spe*I in 3′ junctions. The resulting fusion was cloned into the Gateway vector pK2GW7 under the control of a 35S promoter.

The *ERD2*-CFP construct was previously described in Chatre et al. (2005). Aleu-GFP was previously described (Humair et al., 2001), and a CFP version was made by replacing the GFP6 with an enhanced CFP sequence. The resulting aleu-CFP carries the signal peptide of tobacco (*Nicotiana tabacum*) chitinase and the vacuolar sorting propeptide from petunia (*Petunia hybrida*) aleurain (RTANFADENPIRQVVSDSFHELES) fused to the sequence of the reporter.

Expression in Plants and Confocal Microscopy

For transient expression in tobacco leaves, 3- to 4-week-old plants were used. The construct carried by the binary vector was introduced into plant cells via infiltration of a transformed *Agrobacterium tumefaciens* strain GV3101 p2260 as described previously (Brandizzi et al., 2002). The *Agrobacterium* suspension was inoculated at a density of OD_{600} = 0.3 in the lower epidermis after making a small lesion to facilitate the infiltration. Plants were kept in the dark during expression to allow optimal visualization of vacuolar labeling. We observed the fluorescence 24 to 72 h after transient expression in tobacco epidermal cells from a small leaf piece cut off the plant and mounted in water between slide and cover slip.

Arabidopsis (ecotype Columbia) was transformed with the floral dip method (Clough and Bent, 1998) using the *Agrobacterium* strain GV3101 p2260.

We used either a Leica TCS sp2 (Platform for Cell Imaging of Haute-Normandie PRIMACEN) or an inverse 1 axiovert 200M Zeiss/LSM 510 META confocal microscope (Montpellier RIO imaging platform). For imaging of the coexpression of CFP and GFP6, we used a sequential mode with the 458- and 488-nm laser excitation lines from this microscope. In more detail, the 458- and 488-nm lines were alternatively switched on to detect the CFP fluorescence (from 460 to 485 nm) and the GFP6 fluorescence (from 509 to 602 nm), respectively. The laser power was set to the minimum required for a sharp but not saturating signal, and appropriate controls were made to ensure there was no bleed-through from one channel to the other. That is, we ensured that the signal collected for one fluorochrome remains unchanged when the laser line used to excite the second fluorochrome was switched off. Images were mounted using Adobe Photoshop 7.0 software.

Quantification of Fluorescent Signal

Fluorescence was analyzed using the software provided with the confocal microscope (Leica confocal software 2.5). We aimed to obtain quantitative data on the distribution of fluorescence in three main subcellular locations named punctate structures, plasma membrane, and vacuole. Prior to quantification, we controlled that the fusion protein had reached its final destination by the absence of ER labeling in a confocal section through the nucleus. We first acquired a z-series of transformed cells, with a 1-μm z-step. Laser power was set manually for each single cell at the most fluorescent section to get the maximum signal but just below the saturation level. This setting ensures that the fluorescence signal is optimal but linear and comparable within different sections of a given cell. Regions of interest (ROIs) were then drawn manually at different locations and in different sections of the z-series. ROIs were drawn to contain only fluorescent signal from the subcellular location chosen: punctate structure, plasma membrane, or vacuole content. The mean intensity of fluorescence was measured for each ROI. This measurement was repeated at least five times for one cell, within different z-sections. We repeated measurements on 6 to 10 z-series coming from three independent transient expressions. The relative distribution of signal within spots, vacuole, and plasma membrane was then expressed setting arbitrarily 100% as being the sum of the three types of intensity measured.

Plant Culture and Drug Treatments

Arabidospis plants (Columbia) expressing Pro35S:citrine-*AtVSR4* (this study) or LTi6a-GFP (Cutler et al., 2000) were grown for a week on plates

containing half-strength Murashige and Skoog medium. Drugs were applied by transferring 1-week-old plantlets from the plate on a drop of diluted chemicals. BFA (Sigma-Aldrich) and cycloheximide (Sigma-Aldrich) were both used at a concentration of 50 μM for times indicated in Results (10 to 60 min). Dilution was made freshly from a 1000× stock solution in DMSO.

Accession Numbers

Sequence data from this article can be found in the Arabidopsis Genome Initiative or GenBank/EMBL databases under the following accession numbers: U79958 for pea *BP80*, At2g14720 for *VSR4*, At2g14740 for *VSR3*, and At3g52850 for *VSR1*/At *ELP*.

Supplemental Data

The following materials are available in the online version of this article.

Supplemental Figure 1. Expression of PS1 Fusion Protein in Tobacco Plants.

Supplemental Figure 2. *Arabidopsis* Stably Expressing the Construct Citrine-*AtVSR*4 Produce the Fusion Protein in a Similar Amount Than the Native Homolog.

Supplemental Methods. Immunolabeling Analysis.

Supplemental References.

ACKNOWLEDGMENTS

This work was supported by the Swiss National Science Foundation, Grants 31-46926.96 et 3100-113789 (to J.-M.N.), and by a University of Rouen PhD grant (to B.S.-J.).

Received October 16, 2009; revised June 24, 2010; accepted August 5, 2010; published August 31, 2010.

REFERENCES

Ahmed, S.U., Bar-Peled, M., and Raikhel, N.V. (1997). Cloning and subcellular location of an *Arabidopsis* receptor-like protein that shares common features with protein-sorting receptors of eukaryotic cells. Plant Physiol. **114:** 325–336.

Ahmed, S.U., Rojo, E., Kovaleva, V., Venkataraman, S., Dombrowski, J.E., Matsuoka, K., and Raikhel, N.V. (2000). The plant vacuolar sorting receptor AtELP is involved in transport of NH_2-terminal propeptide-containing vacuolar proteins in *Arabidopsis thaliana*. J. Cell Biol. **149:** 1335–1344.

Anderson, R., and Orci, L. (1988). A view of acidic intracellular compartments. J. Cell Biol. **106:** 539–543.

Batoko, H., Zheng, H.-Q., Hawes, C., and Moore, I. (2000). A Rab1 GTPase is required for transport between endoplasmic reticulum and Golgi apparatus and for normal Golgi movement in plants. Plant Cell **12:** 2201–2217.

Blom, N., Gammeltoft, S., and Brunak, S. (1999). Sequence- and structure-based prediction of eukaryotic protein phosphorylation sites. J. Mol. Biol. **294:** 1351–1362.

Bonifacino, J., and Traub, L. (2003). Signals for sorting of transmembrane proteins to endosomes and lysosomes. Annu. Rev. Biochem. **72:** 395–447.

Brandizzi, F., Frangne, N., Marc-Martin, S., Hawes, C., Neuhaus, J.-M., and Paris, N. (2002). In plants the destination for single pass membrane proteins is markedly influenced by the length of the hydrophobic domain. Plant Cell **14:** 1077–1092.

Chatre, L., Brandizzi, F., Hocquellet, A., Hawes, C., and Moreau, P. (2005). Sec22 and Memb11 are v-SNAREs of the anterograde endoplasmic reticulum-Golgi pathway in tobacco leaf epidermal cells. Plant Physiol. **139:** 1244–1254.

Clough, S.J., and Bent, A.F. (1998). Floral dip: a simplified method for Agrobacterium-mediated transformation of *Arabidopsis thaliana*. Plant J. **16:** 735–743.

Cormack, B.P., Valdivia, R.H., and Falkow, S. (1996). FACS-optimized mutants of the green fluorescent protein (GFP). Gene **173:** 33–38.

Craddock, C., Hunter, P., Szakacs, E., Hinz, G., Robinson, D., and Frigerio, L. (2008). Lack of a vacuolar sorting receptor leads to non-specific missorting of soluble vacuolar proteins in *Arabidopsis* seeds. Traffic **9:** 408–416.

Cutler, S.R., Ehrhardt, D.W., Griffitts, J.S., and Somerville, C.R. (2000). Random GFP: cDNA fusions enable visualization of subcellular structures in cells of *Arabidopsis* at a high frequency. Proc. Natl. Acad. Sci. USA **97:** 3718–3723.

daSilva, L., Foresti, O., and Denecke, J. (2006). Targeting of the plant vacuolar sorting receptor BP80 is dependent on multiple sorting signals in the cytosolic tail. Plant Cell **18:** 1477–1497.

daSilva, L.L., Taylor, J.P., Hadlington, J.L., Hanton, S.L., Snowden, C.J., Fox, S.J., Foresti, O., Brandizzi, F., and Denecke, J. (2005). Receptor salvage from the prevacuolar compartment is essential for efficient vacuolar protein targeting. Plant Cell **17:** 132–148.

Dettmer, J., Hong-Hermesdorf, A., Stierhof, Y.-D., and Schumacher, K. (2006). Vacuolar H^+-ATPase activity is required for endocytic and secretory trafficking in *Arabidopsis.* Plant Cell **18:** 715–730.

Dhonukshe, P., Aniento, F., Hwang, I., Robinson, D., Mravec, J., Stierhof, Y., and Friml, J. (2007). Clathrin-mediated constitutive endocytosis of PIN auxin efflux carriers in *Arabidopsis.* Curr. Biol. **17:** 520–527.

Di Sansebastiano, G.-P., Paris, N., Marc-Martin, S., and Neuhaus, J.-M. (2001). Regeneration of a lytic central vacuole and of neutral peripheral vacuoles can be visualised by GFP targeted to either type of vacuoles. Plant Physiol. **126:** 78–86.

Flückiger, R., De Caroli, M., Piro, G., Dalessandro, G., Neuhaus, J.-M., and Di Sansebastiano, G.-P. (2003). Vacuolar system distribution in *Arabidopsis* tissues, visualized using GFP fusion proteins. J. Exp. Bot. **54:** 1577–1584.

Gao, D., Knight, M., Trewavas, A., Sattelmacher, B., and Plieth, C. (2004). Self-reporting *Arabidopsis* expressing pH and [Ca2+] indicators unveil ion dynamics in the cytoplasm and in the apoplast under abiotic stress. Plant Physiol. **134:** 898–908.

Geldner, N., and Robatzek, S. (2008). Plant receptors go endosomal: A moving view on signal transduction. Plant Physiol. **147:** 1565–1574.

Ghosh, P., Dahms, N., and Kornfeld, S. (2003). Mannose 6-phosphate receptors: New twists in the tale. Nat. Rev. Mol. Cell Biol. **4:** 202–213.

Griesbeck, O., Baird, G.S., Campbell, R.E., Zacharias, D.A., and Tsien, R.Y. (2001). Reducing the environmental sensitivity of yellow fluorescent protein. J. Biol. Chem. **276:** 29188–29194.

Grignon, C., and Sentenac, H. (1991). pH and ionic conditions in the apoplast. Annu. Rev. Plant Physiol. Plant Mol. Biol. **42:** 103–128.

Happel, N., Höning, S., Neuhaus, J.-M., Paris, N., Robinson, D.G., and Holstein, S.E.H. (2004). *Arabidopsis* μA-adaptin interacts with the tyrosine motif of the vacuolar sorting receptor VSR-PS1. Plant J. **37:** 678–693.

Hinz, G., Colanesi, S., Hillmer, S., Rogers, J., and Robinson, D. (2007). Localization of vacuolar transport receptors and cargo proteins in the Golgi apparatus of developing *Arabidopsis* embryos. Traffic **8:** 1452–1464.

Hohl, I., Robinson, D.G., Chrispeels, M.J., and Hinz, G. (1996). Transport of storage proteins to the vacuole is mediated by vesicles without a clathrin coat. J. Cell Sci. **109:** 2539–2550.

Humair, D., Hernández Felipe, D., Neuhaus, J.-M., and Paris, N. (2001). Demonstration in yeast of the function of BP-80, a putative plant vacuolar sorting receptor. Plant Cell **13:** 781–792.

Kirsch, T., Paris, N., Butler, J.M., Beevers, L., and Rogers, J.C. (1994). Purification and initial characterization of a potential plant vacuolar targeting receptor. Proc. Natl. Acad. Sci. USA **91:** 3403–3407.

Kotzer, A.M., Brandizzi, F., Neumann, U., Paris, N., Moore, I., and Hawes, C. (2004). *At*RabF2b (Ara7) acts on the vacuolar trafficking pathway in tobacco epidermal cells. J. Cell Sci. **117:** 6377–6389.

Lam, S., Siu, C., Hillmer, S., Jang, S., An, G., Robinson, D., and Jiang, L. (2007). Rice SCAMP1 defines clathrin-coated, trans-Golgi–located tubular-vesicular structures as an early endosome in tobacco BY-2 cells. Plant Cell **19:** 296–319.

Laval, V., Chabannes, M., Carrière, M., Canut, H., Barre, A., Rougé, P., Pont-Lezica, R., and Galaud, J.-P. (1999). A family of *Arabidopsis* plasma membrane receptors presenting animal β-integrin domains. Biochim. Biophys. Acta **1435:** 61–70.

Laval, V., Masclaux, F., Serin, A., Carrière, M., Roldan, C., Devic, M., Pont-Lezica, R.F., and Galaud, J.-P. (2003). Seed germination is blocked in *Arabidopsis* putative (atbp80) antisense transformants. J. Exp. Bot. **54:** 213–221.

Leborgne-Castel, N., Lherminier, J., Der, C., Fromentin, J., Houot, V., and Simon-Plas, F. (2008). The plant defense elicitor cryptogein stimulates clathrin-mediated endocytosis correlated with reactive oxygen species production in bright yellow-2 tobacco cells. Plant Physiol. **146:** 1255–1266.

Lee, G.-J., Kim, H., Kang, H., Jang, M., Lee, D., Lee, S., and Hwang, I. (2007). EpsinR2 interacts with clathrin, adaptor protein-3, AtVTI12, and phosphatidylinositol-3-phosphate. Implications for EpsinR2 function in protein trafficking in plant cells. Plant Physiol. **143:** 1561–1575.

Lee, I., Doray, B., Govero, J., and Kornfeld, S. (2008). Binding of cargo sorting signals to AP-1 enhances its association with ADP ribosylation factor 1-GTP. J. Cell Biol. **180:** 467–472.

Li, Y.-B., Rogers, S.W., Tse, Y.C., Lo, S.W., Sun, S.S.M., Jauh, G.-Y., and Jiang, L. (2002). BP-80 and homologs are concentrated on post-Golgi, probable lytic prevacuolar compartments. Plant Cell Physiol. **43:** 726–742.

Matsuoka, K., Higuchi, T., Maeshima, M., and Nakamura, K. (1997). A vacuolar-type H^+-ATPase in a nonvacuolar organelle is required for the sorting of soluble vacuolar protein precursors in tobacco cells. Plant Cell **9:** 533–546.

Miesenböck, G., De Angelis, D., and Rothman, J. (1998). Visualizing secretion and synaptic transmission with pH-sensitive green fluorescent proteins. Nature **394:** 192–195.

Neuhaus, J.-M., and Paris, N. (2006). Plant vacuoles: From biogenesis to function. In Plant Endocytosis, J. Samaj, F. Baluska, and D. Menzel, eds (Berlin, Heidelberg, Germany: Springer-Verlag), pp. 63–82.

Niemes, S., Labs, M., Scheuring, D., Krueger, F., Langhans, M., Jesenofsky, B., Robinson, D., and Pimpl, P. (2010a). Sorting of plant vacuolar proteins is initiated in the ER. Plant J. **62:** 601–614.

Niemes, S., Langhans, M., Viotti, C., Scheuring, D., Yan, M., Jiang, L., Hillmer, H., Robinson, D., and Pimpl, P. (2010b). Retromer recycles vacuolar sorting receptors from the trans-Golgi network. Plant J. **61:** 107–121.

Oliviusson, P., Heinzerling, O., Hillmer, S., Hinz, G., Tse, Y.C., Jiang, L., and Robinson, D.G. (2006). Plant retromer, localized to the prevacuolar compartment and microvesicles in *Arabidopsis*, may interact with vacuolar sorting receptors. Plant Cell **18:** 1239–1252.

Ortiz-Zapater, E., Soriano-Ortega, E., Jesús Marcote, M., Ortiz-Masiá, D., and Aniento, F. (2006). Trafficking of the human transferrin receptor in plant cells: Effects of tyrphostin A23 and brefeldin A. Plant J. **48:** 757–770.

Otegui, M., Herder, R., Schulze, J., Jung, R., and Staehelin, L. (2006). The proteolytic processing of seed storage proteins in *Arabidopsis* embryo cells starts in the multivesicular bodies. Plant Cell **18:** 2567–2581.

Paris, N., Rogers, S.W., Jiang, L., Kirsch, T., Beevers, L., Phillips, T.E., and Rogers, J.C. (1997). Molecular cloning and further characterization of a probable plant vacuolar sorting receptor. Plant Physiol. **115:** 29–39.

Park, J., Oufattole, M., and Rogers, J. (2007). Golgi-mediated vacuolar sorting in plant cells: RMR proteins are sorting receptors for the protein aggregation/membrane internalization pathway. Plant Sci. **172:** 728–745.

Perret, E., Lakkaraju, A., Deborde, S., Schreiner, R., and Rodriguez-Boulan, E. (2005). Evolving endosomes: How many varieties and why? Curr. Opin. Cell Biol. **17:** 423–434.

Pitcher, C., Honing, S., Fingerhut, A., Bowers, K., and Marsh, M. (1999). Cluster of differentiation antigen 4 (CD4) endocytosis and adaptor complex binding require activation of the CD4 endocytosis signal by serine phosphorylation. Mol. Biol. Cell **10:** 677–691.

Pond, L., Kuhn, L., Teyton, L., Schutze, M.-P., Tainer, J., Jackson, M., and Peterson, P. (1995). A role for acidic residues in di-leucine motif-based targeting to the endocytic pathway. J. Biol. Chem. **270:** 19989–19997.

Robinson, D., Jiang, L., and Schumacher, K. (2008). The endosomal system of plants: Charting new and familiar territories. Plant Physiol. **147:** 1482–1492.

Sanderfoot, A.A., Ahmed, S.U., Marty-Mazars, D., Rapoport, I., Kirchhausen, T., Marty, F., and Raikhel, N.V. (1998). A putative vacuolar cargo receptor partially colocalizes with atPEP12p on a prevacuolar compartment in *Arabidopsis* roots. Proc. Natl. Acad. Sci. USA **95:** 9920–9925.

Sandoval, I., Martinez-Arca, S., Valdueza, J., Palacios, S., and Holman, G. (2000). Distinct reading of different structural determinants modulates the dileucine-mediated transport steps of the lysosomal membrane protein LIMPII and the insulin-sensitive glucose transporter GLUT4. J. Biol. Chem. **275:** 39874–39885.

Seaman, M.N.J. (2007). Identification of a novel conserved sorting motif required for retromer-mediated endosome-to-TGN retrieval. J. Cell Sci. **120:** 2378–2389.

Shimada, T., Fuji, K., Tamura, K., Kondo, M., Nishimura, M., and Hara-Nishimura, I. (2003). Vacuolar sorting receptor for seed storage proteins in *Arabidopsis thaliana.* Proc. Natl. Acad. Sci. USA **100:** 16095–16100.

Shimada, T., Koumoto, Y., Li, L., Yamazaki, M., Kondo, M., Nishimura, M., and Hara-Nishimura, I. (2006). AtVPS29, a putative component of a retromer complex, is required for the efficient sorting of seed storage proteins. Plant Cell Physiol. **47:** 1187–1194.

Shimada, T., Kuroyanagi, M., Nishimura, M., and Hara-Nishimura, I. (1997). A pumpkin 72-kDa membrane protein of precursor-accumulating vesicles has characteristics of a vacuolar sorting receptor. Plant Cell Physiol. **38:** 1414–1420.

Song, J., Lee, M., Lee, G.-J., Cheol Min Yoo, C., and Hwang, I. (2006). *Arabidopsis* EPSIN1 plays an important role in vacuolar trafficking of soluble cargo proteins in plant cells via interactions with clathrin, AP-1, VTI11, and VSR1. Plant Cell **18:** 2258–2274.

Takano, J., Tanaka, M., Toyoda, A., Miwa, K., Kasai, K., Fuji, K., Onouchi, H., Naito, S., and Fujiwara, T. (2010). Polar localization and degradation of *Arabidopsis* boron transporters through distinct trafficking pathways. Proc. Natl. Acad. Sci. USA **107:** 5220–5225.

Traub, L. (2005). Common principles in clathrin-mediated sorting at the Golgi and the plasma membrane. Biochim. Biophys.Acta **1744:** 415–437.

Tse, Y.C., Mo, B., Hillmer, S., Zhao, M., Lo, S.W., Robinson, D.G., and Jiang, L. (2004). Identification of multivesicular bodies as prevacuolar compartments in *Nicotiana tabacum* BY2 cells. Plant Cell **16:** 672–693.

von Essen, M., Menné, C., Nielsen, B., Lauritsen, J., Dietrich, J., Andersen, P., Karjalainen, K., Ødum, N., and Geisler, C. (2002). The CD3 γ leucine-based receptor-sorting motif is required for efficient ligand-mediated TCR down-regulation. J. Immunol. **168:** 4519–4523.

Watanabe, E., Shimada, T., Kuroyanagi, M., Nishimura, M., and Hara-Nishimura, I. (2002). Calcium-mediated association of a putative vacuolar sorting receptor PV72 with a propeptide of 2S albumin. J. Biol. Chem. **277:** 8708–8715.

Watanabe, E., Shimada, T., Tamura, K., Matsushima, R., Koumoto, Y., Nishimura, M., and Hara-Nishimura, I. (2004). An ER-localized form of PV72, a seed-specific vacuolar sorting receptor, interferes the transport of an NPIR-containing proteinase in *Arabidopsis* leaves. Plant Cell Physiol. **45:** 9–17.

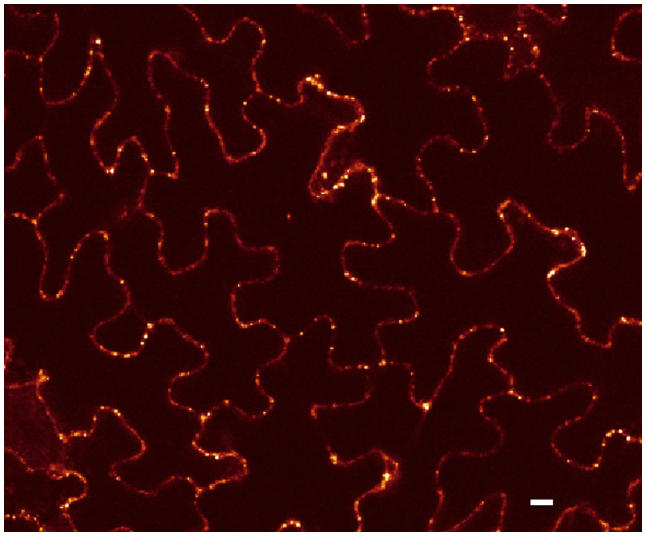

Supplemental Figure 1 : Expression of PS1 fusion protein in tobacco plants.

A stable transformant of tobacco expressing the fusion protein PS1 was grown and young leaves were observed with the confocal microscope.

Scale bar, 10µm

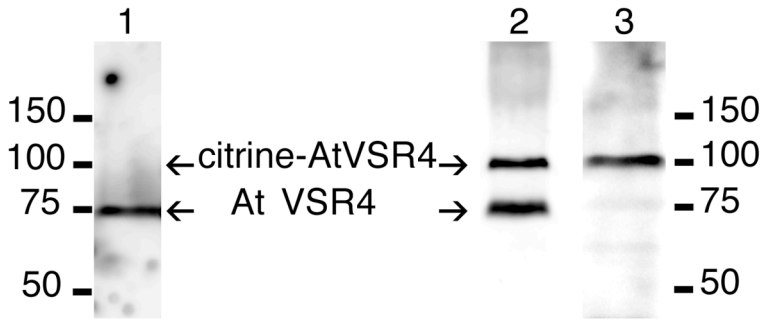

Supplemental Figure 2 : *Arabidopsis* plants expressing stably the construct citrine-At*VSR4* produce the fusion protein in a similar amount than the native homologue.

Immunoblots were performed on total proteins from wild type plants (lane 1) or plants expressing citrine-At*VSR4* (lanes 2 and 3). Affinity purified anti-AtVSR4 (lane 1 and 2) or anti-GFP antibodies (lane 3) were used. Positions for At VSR4 (80kDa) and citrine-AtVSR4 (103kDa) are identified with arrows. Quantification of luminescence from the two bands detected in lane 2 indicates 47% of At VSR4 for 53% of citrine-AtVSR4.

Estimated molecular weights are indicated in kDalton.

Supplemental Methods

For immunolabeling analysis, plants were grown for 18 days as described previously (Kilian et al., 2007). More precisely, seeds were grown for 13 d on MS/2 plates and transferred into liquid medium on floating rafts for 5 days in long-day conditions. Expression was checked under confocal microscopy prior to protein extraction. Tissue was rapidly frozen in liquid nitrogen and ground to a fine powder using a pilar and a mortar. Proteins were extracted by boiling for 10 min in loading buffer for SDS-PAGE (Laemmli, 1970). Large aggregates were removed by centrifugating at 13000 g for 10 min. A quantity of 10 µg to 20 µg of total protein was loaded, separated in a 12% SDS gel and transferred to nitrocellulose. As primary antibodies, we used affinity purified IgGs (1µg/mL) raised against a C-terminal peptide from At VSR4 (PEVPNHTNDERA) and anti-GFP (Molecular probes A6455, 1/2000) to identify the fusion protein citrine-AtVSR4. Immunolabelled proteins were revealed using secondary antibodies coupled to horseradish peroxidase (1/2000, Bio-Rad 1721019) and chemiluminescence (Millipore P90720). Signal recovery and measurement was performed using a Fuji LAS-3000 system (exposure times from 10 sec to 60 sec).

Supplemental References

Kilian, J., Whitehead, D., Horak, J., Wanke, D., Weinl, S., Batistic, O., D'Angelo, C., Bornberg-Bauer, E., Kudla, J., and Harter, K. (2007). The AtGenExpress global stress expression data set: protocols, evaluation and model data analysis of UV-B light, drought and cold stress responses. The Plant Journal 50: 347-363.

Laemmli, U.K. (1970). Cleavage of structural proteins during the assembly of the head of bacteriophage T4. Nature 227: 680-685.